Journal of Alloys and Compounds 480 (2009) 893–896

Contents lists available at ScienceDirect

Journal of Alloys and Compounds

journal homepage: www.elsevier.com/locate/jallcom

Optical properties of PbTe and PbSnTe doped with Cr

P.M. Nikolić[a,*], K.M. Paraskevopoulos[b], S.S. Vujatović[a], M.V. Nikolić[c], X. Chatzistavrou[b], E. Pavlidou[b], T. Ivetić[a], V. Blagojević[d], A. Bojičić[a], D. Dinulović[a]

[a] Institute of Technical Sciences of SASA, Knez Mihailova 35/IV, 11000 Belgrade, Serbia
[b] Physics Department, Solid State Section, Aristotle University of Thessaloniki, 54124 Thessaloniki, Greece
[c] Institute for Multidisciplinary Research, Kneza Višeslava 1, 11000 Belgrade, Serbia
[d] Faculty of Electrical Engineering, University of Belgrade, Bulevar Kralja Aleksandra 73, 11000 Belgrade, Serbia

ARTICLE INFO

Article history:
Received 26 December 2008
Accepted 19 February 2009
Available online 4 March 2009

Keywords:
Semiconductors
Impurities in semiconductors
Optical spectroscopy

ABSTRACT

Single crystal samples of PbTe and PbSnTe doped with Cr were made using the Bridgman technique. Far infrared diagrams of PbTe samples doped with 0.4 at.%, 0.8 at.% and 1 at.% Cr and also of $Pb_{0.9}Sn_{0.1}Te$ doped with 0.4 at.%, 0.7 at.% and 1.1 at.% Cr are presented and numerically analyzed. Local modes were determined at about 260 cm^{-1} and 480 cm^{-1} for PbTe doped with Cr and at slightly higher frequencies for PbSnTe doped with Cr. The origin of the local modes was discused about the possible application of the PbSnTe + Cr alloys.

1. Introduction

Lead telluride is a very well-known narrow gap semiconductor, which has been used for the production of lasers and LED diodes. When PbTe is doped with various impurities several unusual effects, which are not present in the undoped semiconductor, can occur [1]. For instance, when PbTe is doped with a group III element, such as In or Ga, that leads to the Fermi level pinning effect, and also the persistent photoconductivity effect at low temperatures [2]. Doping PbTe with a transition metal is also very interesting because the position at the present impurity levels could be tuned by the magnetic field. In PbTe doped with Cr the Fermi level is pinned in the conduction band [3,4] about 100 meV above the conduction band edge. Faraday effect investigations have shown that doping PbTe with Cr up to the concentration of about 0.4 at.% Cr does not affect significantly the effective mass of free carriers, m^*, and the shape of the Fermi surface [5]. Effective mass at the Fermi level was calculated using the Kane model. Negative magnetoresistance in PbTe (Mn, Cr) was observed at temperatures $T < 15$ K [6] while at higher temperatures the magnetoresistance is positive. Optical absorption in PbTe doped with Cr was measured a long time ago [7,8] in the phonon energy range between 0.1 eV and 0.34 eV at room temperature. Analysis of the optical absorption spectra showed that the incorporation of chromium into PbTe produces a slight increase of the energy gap width. In this work we have studied the behavior of PbTe and PbSnTe when they are doped with different amounts of Cr. Far infrared spectra of these semiconductors doped with Cr were measured. The experimental diagrams were numerically analyzed and the optical parameters determined enabling a comparison of the influence of small amounts of Cr dopant on the determined free carrier mobility values for both the PbTe compound and PbSnTe alloy, especially having in mind that relatively recently it was established that PbSnTe IR detectors are more resistant than others to nuclear radiation [9] so investigations on these doped alloys have become interesting again.

2. Experimental

Single crystals of both PbTe and $Pb_{0.9}Sn_{0.1}Te$ doped with a starting composition of 2 at.% Cr were produced using the Bridgman method [10]. High purity elements (6N) Pb, Sn, Te and Cr were used as the source materials. Samples were cut or cleaved from the ingot and then highly polished before they were used for measurements. The content of Pb, Sn, Te and Cr in each sample was determined using EDS analysis. Along the ingots the concentration of Cr decreased from the top to the end of the ingot. This enabled cutting of samples with different contents of Cr. Highly polished samples were used for optical measurements. Far infrared reflectivity spectra of PbTe doped with 0.4 at.%, 0.8 at.% and 1 at.% Cr and also of PbSnTe alloys doped with 0.4 at.%, 0.7 at.% and 1.1 at.% Cr were measured at room temperature using a Bruker IFS-113 V spectrometer. All investigated samples were of the n type.

3. Experimental results and discussion

The room temperature reflectivity spectra, as a function of the wave number, for single crystal PbTe samples doped with 0.4 at.% Cr, 0.8 at.% Cr and 1 at.% Cr are given in Fig. 1a, b and c, respectively. For these three diagrams, plasma frequency was observed at about 153 cm^{-1}, 156 cm^{-1} and 117 cm^{-1}, respectively. The plasma

* Corresponding author. Tel.: +381 11 2027140; fax: +381 11 2185263.
E-mail address: pantelija.nikolic@sanu.ac.rs (P.M. Nikolić).

0925-8388/$ – see front matter © 2009 Elsevier B.V. All rights reserved.
doi:10.1016/j.jallcom.2009.02.067

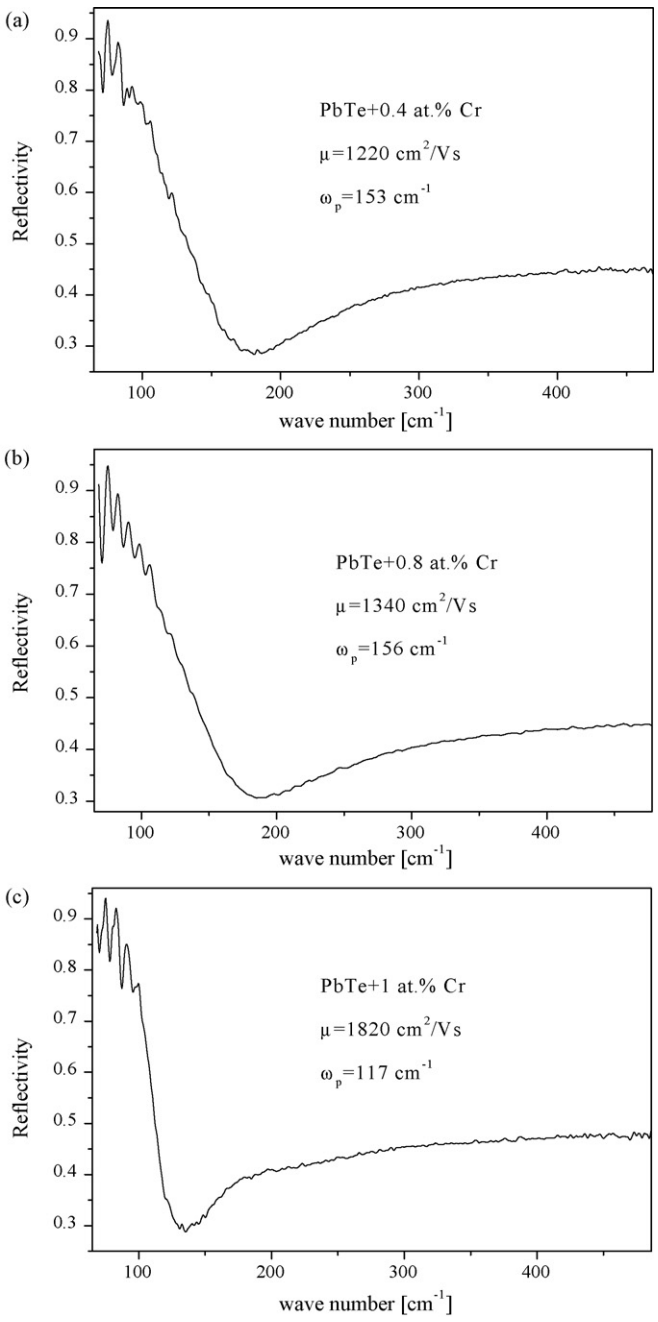

Fig. 1. Room temperature FTIR spectra of PbTe doped with: (a) 0.4 at.% Cr; (b) 0.8 at.% Cr; (c) 1 at.% Cr.

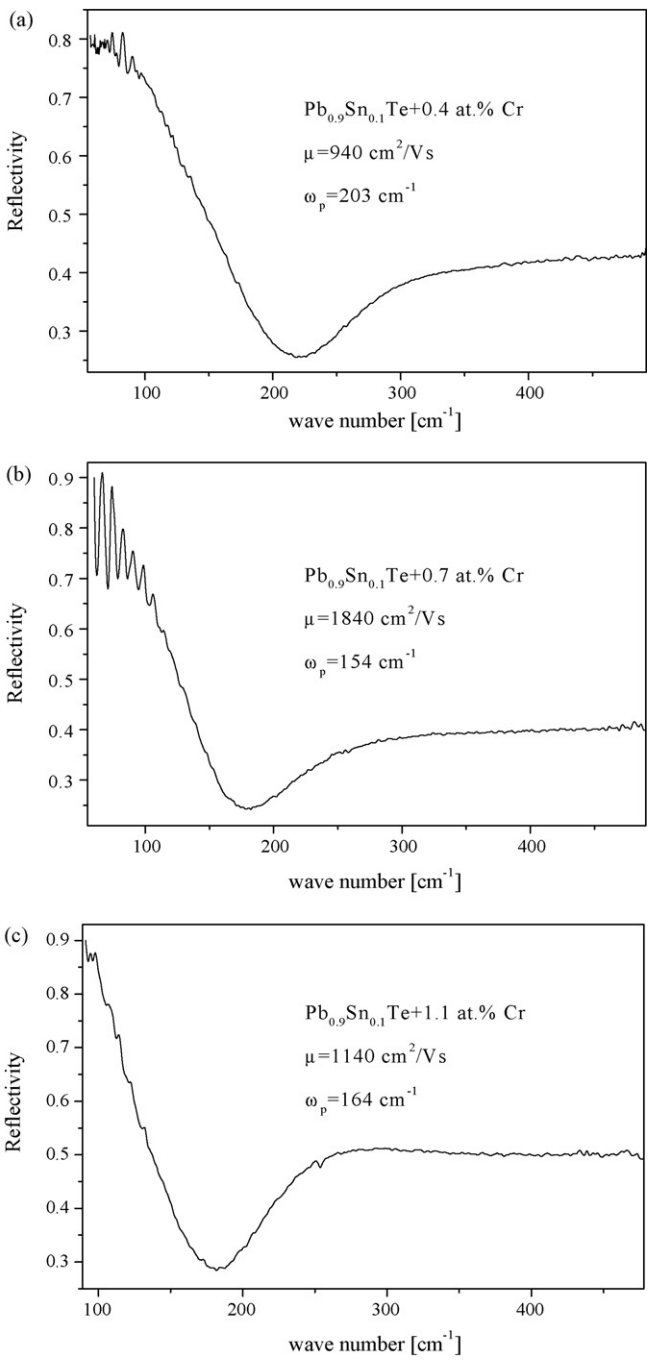

Fig. 2. Room temperature FTIR spectra of $Pb_{0.9}Sn_{0.1}Te$ doped with: (a) 0.4 at.% Cr; (b) 0.7 at.% Cr; (c) 1.1 at.% Cr.

frequency obviously moves to the lowest frequency when the content of Cr is approaching 1 at.% of Cr. For single crystal PbSnTe samples doped with 0.4 at.% Cr, 0.7 at.% Cr and 1.1 at.% Cr the reflectivity diagrams are given in Fig. 2a, b and c, respectively. Their plasma frequencies are a bit higher-at about 203 cm^{-1}, 154 cm^{-1} and 164 cm^{-1}, respectively. All these reflectivity spectra were analyzed with the help of a frequency dependent dielectric function. A four-parameter model [11] where a combined plasmon–LO phonon interaction was taken into account was used [12]:

$$\varepsilon(\omega) = \varepsilon_\infty \frac{\prod_{j=1}^{2}(\omega^2 + i\gamma_{lj}\omega - \omega_{lj}^2)}{\omega(\omega + i\gamma_p)(\omega^2 + i\gamma_t\omega - \omega_t^2)} \cdot \frac{\omega^2 + i\gamma_{LO}\omega - \omega_{LO}^2}{\omega^2 + i\gamma_{TO}\omega - \omega_{TO}^2} \cdot \prod_{n=1}^{r} \frac{(\omega^2 + i\gamma_{Ln}\omega - \omega_{Ln}^2)}{(\omega^2 + i\gamma_{On}\omega - \omega_{On}^2)} \quad (1)$$

where the ω_{lj} and γ_{lj} parameters at the first numerator represent the eigenfrequencies and damping factors of the longitudinal plasmons–phonon (LP + LO) waves, that arise as a result of the interaction of the initial (ω_{LO} PbTe and ω_p) modes. The first denominator's parameters correspond to the transversal (TO) vibrations; γ_p is the damping factor of plasma; ε_∞ is the dielectric high frequency permittivity. The second term in Eq. (1) represents the uncoupled mode of the host crystal, where ω_{LO} and ω_{TO} are the longitudinal and transverse frequencies while γ_{LO} and γ_{TO} are their damping factors. The third term in Eq. (1) represents Cr-impurity modes where ω_{On} and ω_{Ln} are characteristic transverse and longitu-

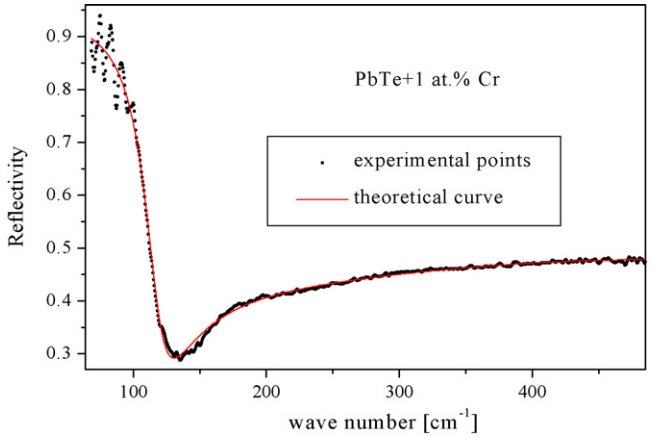

Fig. 3. Measured (circles) and calculated (full line) infrared reflectivity spectrum of PbTe doped with 1 at.% Cr.

dinal frequencies, respectively, and γ_{On} and γ_{Ln} are their damping factors. The plasma wave numbers were calculated using the following equation [12]:

$$\omega_p = \frac{\omega_{l1} \cdot \omega_{l2}}{\omega_t}. \quad (2)$$

Since the reflectivity spectra were measured down to 50 cm^{-1} the transversal phonon mode ω_t was taken from the literature [13] to be 32 cm^{-1}. The starting values of the ε_∞ were calculated using the equation:

$$\varepsilon_\infty = \left(\frac{1+\sqrt{R_\infty}}{1-\sqrt{R_\infty}}\right)^2 \quad (3)$$

where R_∞ is the experimental value of the reflection coefficient at the upper limit of the wave number measured interval. For the fitting procedure the starting values of all parameters were previously determined using Kramers Krönig analysis [14]. As an example, a fitting spectrum of sample PbTe doped with 1 at.% Cr is given in Fig. 3. The values of the parameters calculated using Eqs. (1) and (2) for all samples are given in Table 1. The values of their error bars are smaller than 1 cm^{-1}. In the same table the values of optical mobility of free carriers calculated using the method of Moss et al. [15] are also given. One can see that PbTe + Cr samples with the highest concentration of Cr (1 at.%) have the lowest plasma frequency that is just below 120 cm^{-1}. When the concentration of Cr decreased the plasma minimum moved to a higher wave number-above 150 cm^{-1}. The optical free carrier mobility was the highest for the lowest frequency at the plasma minimum. It was above 1800 $cm^2\ V^{-1}\ s^{-1}$.

Table 1
Optical parameters of phonons and plasmons obtained by oscillator fitting of PbTe and PbSnTe + Cr reflection spectra at room temperature. All values are given in cm^{-1}, except μ_n that is in $cm^2\ V^{-1}\ s^{-1}$.

PbTe + Cr	0.4 at.%	0.8 at.%	1 at.%	PbSnTe + Cr	0.4 at.%	0.7 at.%	1.1 at.%
ω_p	153	156	117	ω_p	203	154	164
γ_p	76	72	30	γ_p	92	71	84
ω_{01}	260	260	260	ω_{01}	276	274	267
γ_{01}	278	187	322	γ_{01}	139	172	94
ω_{L1}	265	265	265	ω_{L1}	286	289	285
γ_{L1}	279	173	245	γ_{L1}	317	236	214
ω_{02}	480	480	480	ω_{02}	491	492	490
γ_{02}	490	754	478	γ_{02}	264	1695	437
ω_{L2}	540	540	540	ω_{L2}	586	586	586
γ_{L2}	492	776	552	γ_{L2}	432	1479	624
μ_n	1220	1340	1820	μ_n	940	1840	1140

Table 2
Electronic structure of: Cr, Mn, Fe, Co and Ni.

No.	Element	Noinozied atom	Ground state	e^{1+}	e^{2+}	e^{3+}
24	Cr	$3d^5 4s$	$(^7S_3)$	$3d^5(^6S_{5/2})$	$3d^4(^5D_o)$	$3d^3(^4F_{3/2})$
25	Mn	$3d^5 4s^2$	$(^6S_{5/2})$	$3d^5 4s(^7S_3)$	$3d^5(^6S_{5/2})$	$3d^4(^5D_o)$
26	Fe	$3d^6 4s^2$	$(^6D_4)$	$3d^6 4s(^6D_{9/2})$	$3d^6(^5D_4)$	$3d^5(^6S_{5/2})$
27	Co	$3d^7 4s^2$	$(^4F_{9/2})$	$3d^7 4s(^3F_4)$	$3d^7(^4F_{9/2})$	$3d^6(^5D_4)$
28	Ni	$3d^8 4s^2$	$(^3F_4)$	$3d^9(^2D_{5/2})$	$3d^8(^3F_4)$	$3d^7(^4F_{9/2})$

For PbSnTe doped with Cr the highest free carrier mobility was very similar (1840 $cm^2\ V^{-1}\ s^{-1}$) when the concentration of Cr was 0.7 at.% and when the plasma minimum was the lowest (154 cm^{-1}). But when the concentration of Cr was either higher or lower the values of free carrier mobility decreased. One should notice that all these values for PbSnTe doped with Cr are very similar to the properties of PbTe + Cr. They are better than literature values of mobility for pure PbSnTe [16]. Obviously Cr as a dopant improves the properties of PbSnTe a lot. During the fitting procedure of reflectivity spectra, given in both Figs. 1 and 2 we realized that they were fitted the best when we supposed the existence of two local Cr modes. For PbTe + Cr they were at about 260 cm^{-1} and 480 cm^{-1} while for PbSnTe + Cr they were at a bit higher frequencies: about 286 cm^{-1} and 490 cm^{-1}.

Now one can consider how many local modes of Cr could exist in PbTe. Since Cr belongs to group of transition metals together with: Mn, Fe, Co and Ni we could observe the electronic structure of nonionized and ionized states for these metals, which is given in Table 2. The electronic structure of Cr and Mn are rather similar, but as far as we know, literature data of optical properties of PbTe doped with Mn is limited [17].

Only one local Mn mode at about 50 cm^{-1} was observed. It is interesting to mention here that also for PbTe doped with Ni we clearly observed only one mode [18] in the same low frequency range at about 60 cm^{-1}. For this doped semiconductor three more local modes were observed [19] at: 130 cm^{-1}, 165 cm^{-1} and 190 cm^{-1}. The conclusion was reached that the mode at 190 cm^{-1} corresponded to Ni^{3+}; mode at about 130 cm^{-1} to Ni^{2+} and the mode at about 165 cm^{-1} corresponded to Ni^{1+}. In another paper on PbMnTe doped with Cr [20] the existence of only two local Cr modes in PbMnTe was noted, e.g. Cr^{2+} and Cr^{3+}. So, in our case we could assume that our two modes given in Table 1 at about 260 cm^{-1} and 480 cm^{-1} could correspond to Cr^{3+} and Cr^{2+}, respectively. Then a question could arise what about the Cr^{1+} ion? For the determination of this Cr impurity mode, we have used previously obtained results by the extension of a linear diatomic chain model for the determination of a local mode frequency in a real crystal [21]. Then the position of the impurity mode could be calculated using the simple formula described in [22]:

$$\omega_{0Cr} = \omega_{TOPbTe}\sqrt{\frac{M_{Pb}}{M_{Cr}}} \quad (4)$$

where M_{Pb} and M_{Cr} are the mass of the host crystal and of the impurity atom, respectively, and ω_{TOPbTe} is the transverse optical mode frequency of PbTe. The calculated value of this impurity mode, at room temperature, is 63.8 cm^{-1}. To check this value we have measured far infrared reflection spectra of a PbTe + 1.4 at.% Cr single crystal sample in the frequency range below 50 cm^{-1}, which is given in Fig. 4. The spectra were measured at 300 K and about 200 K where peaks in the range below 50 cm^{-1} were better exposed and the low frequency Cr^{1+} mode was confirmed to be at about 64 cm^{-1}. A similar discussion on impurity modes and their origin could be applied to PbSnTe samples doped with Cr. It is more important to emphasize here that PbSnTe alloys doped with Cr have a very similar free carrier mobility to single crystal samples of PbTe doped with Cr

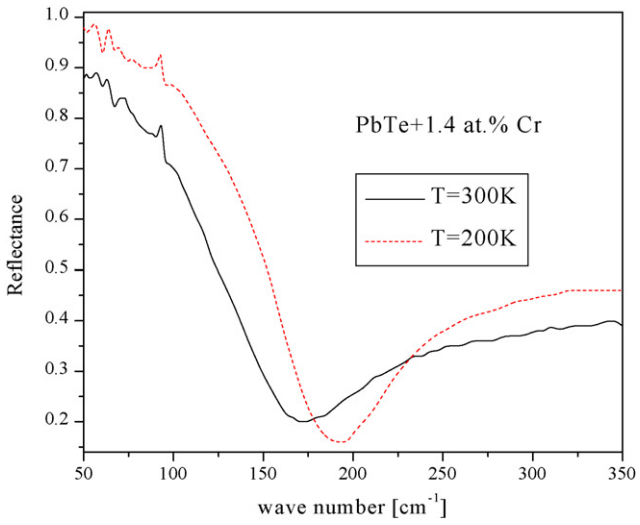

Fig. 4. Reflectivity spectra of PbTe + 1.4 at.% Cr sample measured at 300 K (full line) and about 200 K (dashed line).

(Table 1). Knowing that pure PbSnTe alloys have a much smaller energy gap compared with PbTe it is obvious that PbSnTe doped with Cr has an improved electrical characteristic especially the free carrier mobility and could be used for the production of high quality sensitive far infrared detectors that are stable with respect to the action of hard radiation, for example in infrared astronomy.

4. Conclusion

In this work far infrared spectra of chromium doped PbTe and PbSnTe single crystals have been shown and numerically analyzed. The infrared spectra have been fitted using a modified plasmon–phonon interaction model with three additional oscillators at about 64 cm^{-1}, 260 cm^{-1} and 480 cm^{-1}, which represent local Cr-impurity mode behavior. For PbSnTe single crystal samples doped with about 0.7 at.% Cr we obtained the highest free carrier mobility. This means that the studied PbSnTe + Cr materials could be used for making infrared devices stable for nuclear radiation, which could be very useful in modern astronomy.

Acknowledgements

This work was performed as part of F130 project of the Serbian Academy of Sciences and Arts.

References

[1] B.A. Akimov, A.V. Dmitriev, D.R. Khokhlov, L.I. Ryabova, Phys. Stat. Sol. A 137 (1993) 9–55.
[2] B.A. Volkov, L.I. Ryabova, D.R. Khokhlov, Phys.-Usp. 45 (2002) 819–846.
[3] L.M. Kashirskaya, L.I. Ryabova, O.I. Tananaeva, N.A. Shirokova, Sov. Phys. Semicond. 24 (1990) 848–853.
[4] B.A. Akimov, N.A. Lvova, L.I. Ryabova, Phys. Rev. B 58 (1998-II) 10430–10434.
[5] M. Raturszek, M.J. Raturszek, J. Phys. Chem. Solids 46 (1985) 837–840.
[6] A.V. Morozov, A.E. Kozhanov, A.I. Artamkin, E.I. Sly'nko, V.E. Sly'nko, W.D. Dobrovolski, T. Story, D.R. Khokhlov, Semiconductors 38 (2004) 27–30.
[7] M. Baleva, D. Bakoeva, J. Mater. Sci. Lett. 5 (1986) 37–39.
[8] V.D. Vulchev, Bulg. J. Phys. 15 (1988) 56–59.
[9] D.R. Khokhlov, Usp. Fiz. Nauk 176 (2006) 983–986.
[10] B.A. Akimov, A.V. Nikorich, L.I. Ryabova, N.A. Shirokova, Fiz. Tekh. Poluprovodn. 23 (1989) 1019–1024.
[11] F. Gervais, B. Piriou, Phys. Rev. B 10 (1974) 1642–1654.
[12] A.A. Kukharskii, Solid State Commun. 13 (1973) 1761–1765.
[13] S. Takaoka, T. Itoga, K. Murase, Jpn. J. Appl. Phys. 23 (1984) 216–222.
[14] D.M. Moessler, Br. J. Appl. Phys. 16 (1965) 1119–1123, and 1359–1366.
[15] T.S. Moss, T.D.F. Howkins, G.J. Burell, J. Phys. C 1 (1968) 1435–1446.
[16] G. Dionne, J.C. Woolley, Phys. Rev. B 6 (1972) 3898–3913.
[17] J. Trajić, M. Romčević, N. Romčević, S. Nikolić, A. Golubović, S. Djurić, V.N. Nikiforov, J. Alloys Compd. 365 (2004) 89–93.
[18] D. Luković, W. König, V. Blagojević, O. Jakšić, P.M. Nikolić, Mater. Res. Bull. 41 (2006) 367–375.
[19] N. Romčević, J. Trajić, T.A. Kuznetsova, M. Romčević, B. Hadžić, D.R. Khokhlov, J. Alloys Compd. 442 (2007) 324–327.
[20] A.I. Artamkin, A. Kozhanov, M. Arciszewska, W. Dobrowolski, T. Story, E.I. Slynko, V.E. Slynko, D. Khokhlov, Acta Phys. Pol. A 106 (2004) 223–231.
[21] G. Lucovsky, M.H. Brodsky, E. Burstein, Phys. Rev. B 2 (1970) 3295–3302.
[22] S. Venigopalan, A. Petrov, R.R. Galazka, A.K. Ramdas, S. Rodriguez, Phys. Rev. B 25 (1982) 2681–2696.